


Article

Impact of the Atomic Packing Density on the Properties of Nitrogen-Rich Calcium Silicate Oxynitride Glasses

Sharafat Ali 

Department of Built Environment and Energy Technology, School of Engineering, Linnæus University, SE-351 95 Vaxjo, Sweden; sharafat.ali@lnu.se

Abstract: In this work, the impact of the atomic packing density/fractional glass compactness of Ca–Si–O–N glasses on glass transition and crystallization temperatures, glass density, microhardness, molar volume, and refractive index were examined. It was found that the atomic packing density increased with increasing the nitrogen content and decreased with increasing the Ca content in the glass network. Furthermore, density, glass transition and crystallization temperatures, and refractive index, increased with an increasing atomic packing density of the glass, while molar volume increased with decreasing atomic packing density values. The change in hardness with atomic packing density is less clear and suggests that the atomic packing density does not solely control the underlying deformation mechanism. There is indeed competition between densification (favored at low packing density values) and isochoric shear (at larger packing density). Despite that, the effects of nitrogen as a network former and Ca as a modifier are significantly independent. The obtained results indicate that the atomic packing density of the prepared samples linearly depends on many mechanical and optical properties, suggesting that the glass network and cross-linking are proportional to the ionic radius of the Ca and the nitrogen content, respectively.

Keywords: oxynitride glass; atomic packing density; refractive index; hardness; high nitrogen content; high calcium content



Citation: Ali, S. Impact of the Atomic Packing Density on the Properties of Nitrogen-Rich Calcium Silicate Oxynitride Glasses. *Materials* **2022**, *15*, 6054. <https://doi.org/10.3390/ma15176054>

Academic Editor: Konda Gokuldoss Prashanth

Received: 26 July 2022

Accepted: 30 August 2022

Published: 1 September 2022

Publisher's Note: MDPI stays neutral with regard to jurisdictional claims in published maps and institutional affiliations.



Copyright: © 2022 by the author. Licensee MDPI, Basel, Switzerland. This article is an open access article distributed under the terms and conditions of the Creative Commons Attribution (CC BY) license (<https://creativecommons.org/licenses/by/4.0/>).

1. Introduction

It is well-known that the incorporation of nitrogen (N) into the oxide glass network exhibits superior mechanical properties such as toughness, elastic moduli, and microhardness; furthermore, the glass transition temperature (T_g), crystallization temperature (T_c), and refractive index (RI) also significantly increase with N content. These types of trends are most likely due to the partial replacement of two-fold coordinated oxygen atoms with three-fold coordinated N. Such observations have been confirmed using several techniques, including FTIR, X-ray photoelectron spectroscopy (XPS), and nuclear magnetic resonance (NMR) [1,2]. It is also important to mention that the incorporation of N in the glass generally provides a more tightly and highly linked glass network [3–8].

Oxynitride glasses are typically synthesized in a wide range of oxide systems, e.g., silicate, aluminosilicate, boroaluminosilicate, fluoroaluminosilicate, borate, borophosphate, phosphate, phosphosilicate, and phosphoaluminosilicate glasses. Silicon-based oxynitride glasses have been studied most, both from preparation and properties point of view, compared to other oxynitride glasses. These glasses can be prepared by melting mixtures containing glass modifier metal oxide, SiO_2 , and $\text{Si}_3\text{N}_4/\text{AlN}$, yielding glasses with N content up to typically c.a. 25 e/o. Recently, few studies have reported that AE/RE–Si–O–N (where “AE” is alkaline-earth and “RE” is rare-earth) glasses can be formed by incorporating a metal modifier such as metal hydride or even pure metal in the reaction mixture rather than using metal oxides, as typically used with silicon nitride (Si_3N_4) as the N source yielding oxynitride glasses, with N content of up to 60 e/o with exceptional thermal, mechanical, and optical properties [9–16].

For oxide glasses [17–19] as well as for oxynitride glasses [20–24], several studies have shown that many mechanical properties such as elastic properties, hardness, and thermal properties, e.g., glass transition temperature (T_g) and crystallization temperature (T_c), depend on three main factors: (1) the type of *AE/RE* element, (2) the amount of the *AE/RE* in the glass system, and (3) the amount of N. [25,26]. Rouxel et al. [27] discussed the elastic properties of glasses in the light of their short to medium-range structural features (i.e., coordination number, cross-linking between rings, sheets, and chains, the dimensionality of the structural units, and interatomic bonding). It is noteworthy to mention that owing to the unknown of many structural properties such as bond energies, bond lengths, and bond angles, it is difficult to analyze the atomic structure distribution of the glass precisely. Interestingly, few properties, such as atomic packing density/fractional glass compactness, can be associated with the glass properties. The atomic packing density of glass is a measure of how well the ions are packed in the glass. Atomic packing density is not known with high accuracy because ionic radii depend on the fine details of the atomic organization (coordination, valency, affinity with the neighboring atoms). Furthermore, the meaning of an ionic radius is questionable as the interatomic bonds increase, for instance, when more covalent species such as N are introduced. Nevertheless, in general, atomic packing density provides some insight into the trends in properties [27]. In oxide glasses, where the atomic network is built on chiefly ionic bonds, cation field strength (*CFS*) is another useful parameter (for instance, to differentiate glasses which only differ by the nature of the rare-earth oxide introduced); however, the situation is more complicated in the presence of strong covalent bonds as in oxynitride glasses [7].

The addition of N and modifier to a series of Ca–Si–O–N glasses was investigated by Sharafat et al. [12,13,28] and unraveled the effect of N on glass properties. The present work discusses the relationships between the atomic packing density (C_g), molar volume (Mv), density (ρ), glass transition temperature (T_g), Vickers hardness (H_v), and refractive index (RI) of Ca–Si–O–N glasses with varying calcium (Ca) and nitrogen (N) contents.

2. Experimental

In this study, a series of Ca–Si–O–N samples with a high amount of N and modifier were selected, as displayed in Table 1, and the specimen was labeled accordingly, increasing N content in the glass network. In addition, all of the compositions presented in this work are expressed as an equivalent percent [N content in equivalent; $e/o = (3[N] \times 100)/(2[O] + 3[N])$, where [O] and [N] are the atomic concentrations of nitrogen and oxygen, and 3 and 2 are their respective valences]. Oxynitride glasses in the calcium silicon oxynitride system were fabricated by the traditional melt-quenching technique from mixtures of Calcium hydride (purity 98%), purchased from Alfa Aesar GmbH & Co. (Kandel, Germany), and Si_3N_4 and SiO_2 powders purchased from ChemPur GmbH (Karlsruhe, Germany) and ABCR GmbH & Co. (Karlsruhe, Germany), respectively. Subsequently, an equal volume mixture (6 gm batches) of each composition was mixed and ground inside a glove box filled with argon to avoid the oxidation of the mixture. After that, the powders were placed in Nb crucibles and heated up at 1500–1700 °C via a high-temperature furnace. More details on the fabrication and characterizations of the samples can be found in our previously published works [8,20]. The Archimedes method was used to measure the density of the bulk oxynitride glass samples. The weight of each prepared sample was measured five times in water and air to calculate the standard deviation in each measurement. The molar volume (Mv) of the glass sample consisting of i elements was calculated through the following formula:

$$Mv = \frac{\sum_i X_i m_i}{\rho}, \quad (1)$$

where X_i , M_i , and ρ are the mole fraction, molar mass, and the density of the glass, respectively.

Table 1. Data for prepared Ca–Si–O–N glasses, determined glass composition, Ca content in e/o, Si content in e/o, O content in e/o, N content in e/o, X:Si ratio = [O,N]/[Si], number of bridging oxygen (n_{BO}), and average coordination number $\langle n \rangle$.

Glass ID	Glass Composition	Ca/e/o	Si/e/o	O/e/o	N/e/o	X:Si	n_{BO}	$\langle n \rangle$
1	Ca _{3.41} Si ₁₀ O _{19.75} N _{2.45}	14.6	85.4	84.3	15.7	2.22	3.709	2.543
2	Ca _{5.29} Si ₁₀ O _{21.61} N _{2.46}	20.9	79.1	85.4	14.6	2.41	2.582	2.413
3	Ca _{4.90} Si ₁₀ O _{20.17} N _{3.15}	19.7	80.3	81.0	19.0	2.33	3.606	2.470
4	Ca _{6.52} Si ₁₀ O _{20.02} N _{4.43}	24.6	75.4	75.1	24.9	2.45	3.511	2.408
5	Ca _{9.3} Si ₁₀ O _{22.18} N _{4.75}	31.8	68.2	75.7	24.3	2.69	3.365	2.223
6	Ca _{6.67} Si ₁₀ O _{19.47} N _{4.8}	25.0	75.0	73.0	27.0	2.43	3.500	2.415
7	Ca _{11.81} Si ₁₀ O _{22.06} N _{6.50}	37.1	62.9	69.3	30.7	2.86	3.258	2.108
8	Ca _{8.03} Si ₁₀ O _{17.92} N _{6.65}	28.7	71.3	64.2	35.8	2.46	3.424	2.399
10	Ca _{14.65} Si ₁₀ O _{23.12} N _{7.69}	42.0	58.0	67.0	33.0	3.08	3.155	1.935
9	Ca _{9.14} Si ₁₀ O _{17.37} N _{7.84}	31.4	68.6	59.6	40.4	2.52	3.373	2.367
11	Ca _{12.90} Si ₁₀ O _{20.93} N _{7.98}	39.2	60.8	63.6	36.4	2.89	3.216	2.084
12	Ca _{9.94} Si ₁₀ O _{17.73} N _{8.14}	33.2	66.8	59.9	40.1	2.59	3.336	2.319
13	Ca _{12.91} Si ₁₀ O _{20.37} N _{8.36}	39.3	60.7	61.9	38.1	2.87	3.215	2.098
14	Ca _{11.77} Si ₁₀ O _{16.30} N _{10.31}	37.1	62.9	51.3	48.7	2.66	3.259	2.273
15	Ca _{9.74} Si ₁₀ O _{13.57} N _{10.78}	32.8	67.2	45.6	54.4	2.44	3.345	2.459
16	Ca _{10.07} Si ₁₀ O _{12.92} N _{11.40}	33.4	66.6	43.0	57.0	2.43	3.329	2.464
17	Ca _{11.04} Si ₁₀ O _{13.21} N _{11.89}	35.6	64.4	42.0	58.0	2.51	3.289	2.408

The atomic packing density (C_g) of the glasses was obtained from the total theoretical volume of all ions in a mol of glass and the effective molar volume of the glass using the following formula:

$$C_g = \frac{\sum_i X_i V_i N}{Mv}, \quad (2)$$

where N is a constant called Avogadro's number, while V_i is the ion volume of the element "i". V_i , the volume of the ionic species, can be calculated through the ionic radii (r) given by Shannon [29] using the equation.

$$V_i = \frac{4}{3} \pi r^3. \quad (3)$$

A Netzsch STA 409PC instrument was used to measure the thermal properties (T_g and T_c) of the prepared samples. To measure the thermal properties, crushed pieces of prepared glass were placed in Pt cups and heated up to 1350 °C with a ramp rate of 20 °C/min in flowing nitrogen. A Matsuzawa microhardness tester (Model: MXT- α 1 with a pyramid-shaped diamond indenter) was used to measure the microhardness of the glasses at room temperature. Through a series of indentation experiments (10 indentation experiments for each sample) with an indentation load of 300 g, the indentation responses of the polished glasses samples were measured and compared. The hardness was determined using the below expression.

$$H_v = 2P/d^2, \quad (4)$$

where d [m] and P [N] are the average lengths of the indent's diagonal and indentation load, respectively. The Brewster angle (θ_B) approach estimates the RI of polished glass surfaces using the formula

$$RI = \tan(\theta_B). \quad (5)$$

The measurements were carried out using a 640-nm laser.

The relative number of bridging oxygen atoms calculated per glass-forming cation (n_{BO}) is provided by

$$n_{BO} = 4 - \sum_i M_i Z_i / \left(\sum_j F_j \right), \quad (6)$$

where M_i is the atomic fraction, Z_i represents the valency of the i th modifying cation, and F_j is the fraction of the j th glass-forming cation. In the case of oxynitride glasses, the n_{BO} can be calculated by replacing [O] with an equivalent anionic concentration [O*], with [O*] = [O] + 3/2[N], assuming three-fold coordinated N in the glass network. The average coordination number $\langle n \rangle$ was calculated according to the expression

$$\langle n \rangle = 4x_{Si} - 2x_{Ca} + 2(O - Ca) - [Si - Ca + O + N], \quad (7)$$

where Si, Ca, O, and N are respective atomic concentrations in the glass.

3. Results

3.1. Glass Stoichiometry and Morphology

Tables 1 and 2 summarize the compositions and a range of their analyzed property values of the Ca–Si–O–N glasses investigated in this work. All herein reported Ca–Si–O–N glasses were fabricated using fine powder of calcium hydride as a Ca source and X-ray amorphousness. A typical recorded X-ray powder pattern for pure glass is shown in Figure 1a for the glass sample $Ca_{8.03}Si_{10}O_{17.92}N_{6.65}$ (cf. Table 1, sample # 8) with Ca content of 29 e/o and N content of 36 e/o, respectively. It exhibits the characteristic broad diffraction maxima of an amorphous phase. The fabricated samples in the Ca–Si–O–N matrix were mostly black or dark grey, as previously reported for oxynitride glasses in Ca–Si–(Al)–O–N systems [4,12,26,30–33]. The coloration in these glasses is related to the presence of metal silicide and a small number of Si particles. The obtained glasses comprised up to 58 e/o nitrogen and 42 e/o Ca. Some of the glasses have a higher content of glass modifier, i.e., Ca, than glass former, i.e., Si, and thus fall under the category of inverted oxynitride glasses ($Ca/Si > 1$). The glass composition conveys information about its average network polymerization degree through the X:Si (X= O, N) ratio, corresponding to the number of anions per tetrahedral (network forming) cation, see Table 1. X:Si ratios are found to vary between 2.22 to 2.89 and can be associated with the 3D framework and 2D sheet structure built by Q^4 and Q^3 tetrahedra.

The SEM backscattered electron image and high-resolution transmission electron microscopy (HRTEM) image of glass $Ca_{8.03}Si_{10}O_{17.92}N_{6.65}$ (cf. Table 1, sample # 8) displayed in Figure 1b,c reveal homogenous microstructures; furthermore, selected area electron diffraction (SAED) patterns confirmed that the sample was amorphous in nature. The surface topography was investigated on the freshly fractured surfaces by atomic force microscopy (AFM). Figure 1d reveal that the glass has a smooth and uniform surface, and no metallic inclusions or other heterogeneities were detected. The SEM, HRTEM, and AFM observations confirmed that the samples are defect-free and featureless structures, characteristic of non-crystalline materials. X-ray powered diffraction, SEM, HREM, and AFM images reported in Figure 1a–d refer to the $Ca_{8.03}Si_{10}O_{17.92}N_{6.65}$ sample; however, they are representative of all the studied samples.

3.2. Effect of Atomic Packing Density on Bridging Oxygen and Average Coordination Number

The atomic packing density (C_g) has much less effect on bridging oxygen (n_{BO}) and the average coordination number $\langle n \rangle$ (see Tables 1 and 2). Both the number of bridging oxygen and the average coordination number decrease with the increasing atomic packing density of the glass. This observation can be attributed to the fact that as the cross-linking degree of the atomic network increases, i.e., as the average coordination number or as the number of bridging oxygen atoms per silicate tetrahedron is raised, the atomic packing density decreases.

Table 2. Physical properties of Ca–Si–O–N glasses: glass designation, density (ρ), molar volume (Mv), glass compactness (C_g), glass transition temperature (T_g), crystallization temperature (T_c), Vickers hardness (H_v), and refractive index (RI). Numbers in parentheses are estimated standard deviations.

Glass ID	C_g	$\rho/\text{gm}\cdot\text{cm}^{-3}$	$Mv/\text{cm}^3\cdot\text{mol}^{-1}$	$T_g/^\circ\text{C}$	$T_c/^\circ\text{C}$	H_v/GPa	RI
1	0.560	2.85	7.57	820	935	8.2(2)	1.63
2	0.546	2.80	7.92	798	930	7.3(5)	1.62
3	0.551	2.81	7.86	830	970	7.5(4)	1.65
4	0.562	2.93	7.70	885	953	8.8(83)	1.68
5	0.573	3.02	7.70	858	1020	7.4(5)	1.70
6	0.562	2.90	7.81	-	-	7.5(4)	1.69
7	0.588	3.13	7.60	887	1075	7.7(3)	1.74
8	0.571	3.01	7.66	920	1048	9.3(5)	1.72
9	0.573	3.09	7.85	-	-	7.9(3)	1.75
10	0.573	3.03	7.70	955	1074	9.4(8)	1.74
11	0.565	3.02	7.90	912	1040	7.7(5)	1.74
12	0.575	3.02	7.79	948	1054	7.6(3)	1.72
13	0.582	3.11	7.73	935	1045	7.7(4)	1.75
14	0.584	3.09	7.75	967	1050	8.9(3)	1.85
15	0.599	3.12	7.56	1008	1178	9.9(5)	1.92
16	0.622	3.25	7.29	1050	-	10.1(2)	1.94
17	0.618	3.24	7.37	1010	1170	9.6(2)	1.95
Experimental uncertainties	± 0.001	± 0.02	± 0.01	± 5	± 5		± 0.02

3.3. Effect of Atomic Packing Density on Measured Glass Density and Calculated Molar Volume

The atomic packing density (C_g) of the glass is closely related to the N content and is increased with increasing N content in the glass, as shown in Figure 2a. The C_g values vary between 0.546 and 0.622. Generally, oxynitride glasses have higher values of C_g than oxide glasses ($C_g < 0.540$) and lower values than metallic glass $C_g > 0.70$ [13,27].

Measured values of the density of the oxynitride glass samples are demonstrated in Table 2. As can be observed, the density values of the samples varied from 2.80 to 3.25 g/cm³. The density of the glasses is plotted in Figure 2b as a function of glass atomic packing density. The density increases with increasing atomic packing density. A fit of the data to a linear dependence of density on atomic packing density yielded $\rho = -0.42(0.33) + 5.98(0.58) \times [C_g]$, with regression coefficient $R^2 = 0.87$. The density of the Ca–Si–O–N samples exhibits dependence on C_g and chemical composition.

The molar volume value spans 7.29 cm³/mol to 7.92 cm³/mol. The molar volume decreases with increasing the atomic packing density of the glass and increases with increasing the modifier content, in agreement with previously reported data on other oxynitride systems. $Mv = 11.73(0.67) - 7.02(1.15) \times [C_g]$, with regression coefficient $R^2 = 0.69$. The relationship between the compactness and molar volume is shown in Figure 2c.

3.4. Effect of Atomic Packing Density on Glass Transition and Crystallization Temperatures

The glass transition temperature (T_g) of the oxynitride glass samples depends on the N content and structural parameters. The T_g is expected to increase with the N content, M–O bond strengths, glass cross-linking, and C_g . The T_g and T_c for glasses in the Ca–Si–O–N system are summarized in Table 2, and range from 800 °C to 1050 °C, and from 930 °C to

1220 °C for T_g , and T_c , respectively. The average temperature difference between T_g and T_c is approximately 130 °C.

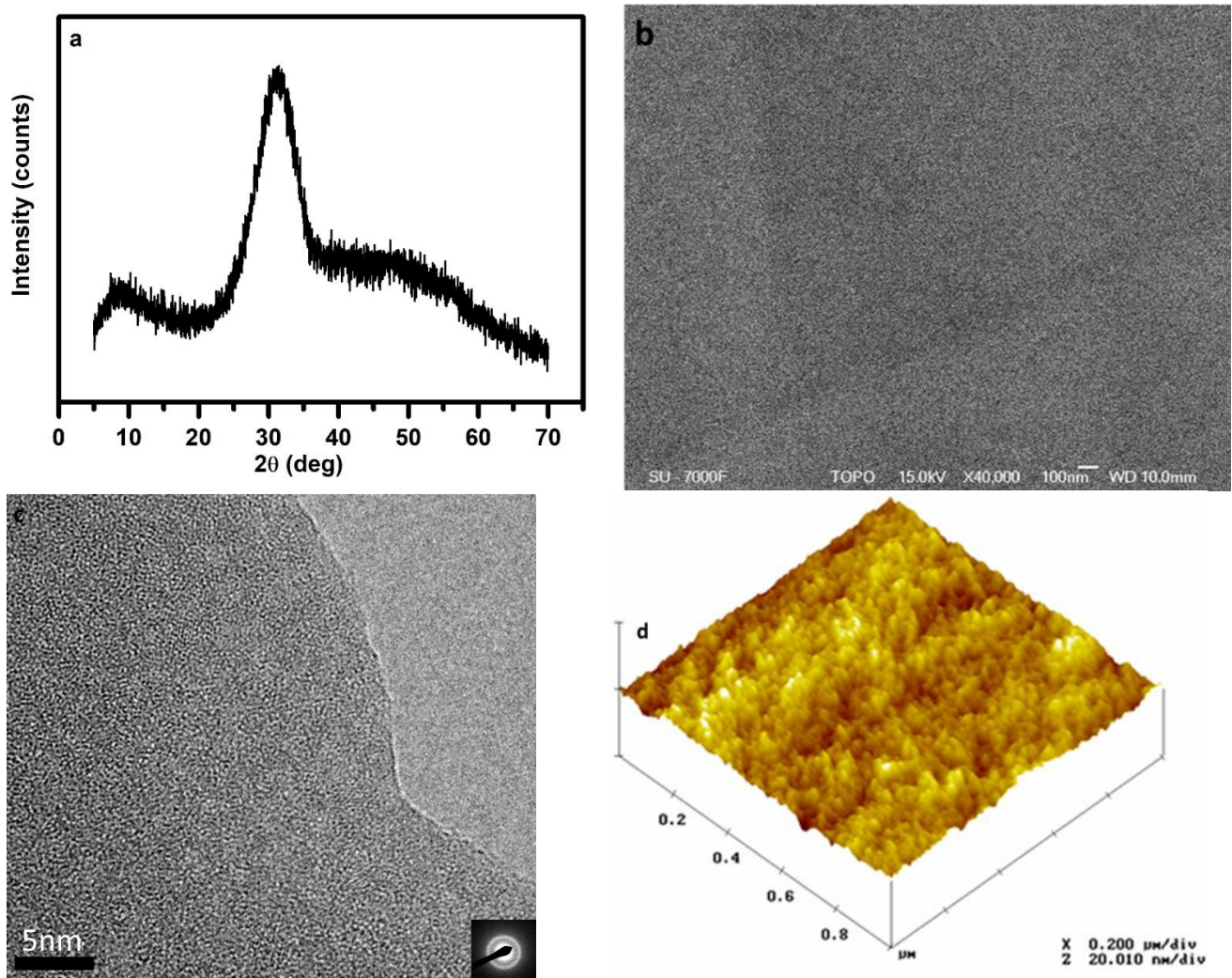


Figure 1. Left panel: (a). XRD pattern (c) high-resolution electron microscopy (HREM) image. Right panel: (b) SEM backscattered electron image and (d) atomic force microscopy image (AFM) of glass sample $\text{Ca}_{8.03}\text{Si}_{10}\text{O}_{17.92}\text{N}_{6.65}$.

Figure 3a show that T_g increases concomitantly with the C_g of the glass since as the addition of N content increases the C_g of the glass, the T_g is expected to increase. The linear dependency between T_g and T_c of the samples due to the C_g yielded $T_g = -800(250) + 2971(438) \times [C_g]$ with regression coefficient $R^2 = 0.77$ and $T_c = -1058(273) + 3650(480) \times [C_g]$ with $R^2 = 0.82$. The dependency of T_g on N content is more obvious, as shown in Figure 3b. Fitting the data to a linear dependence of T_g on N content yielded $T_g = 738(9) + 5(25) \times [N]$, with $R^2 = 97$ and $T_c = 863(23) + 5(62) \times [N]$ with $R^2 = 0.84$.

3.5. Effect of Atomic Packing Density on Hardness

Permanent deformation is characterized by the Vickers hardness (H_v). In Figure 4a,b the mean hardness values of 10 tests are plotted against their corresponding atomic packing density values and N content, respectively, for the Ca–Si–O–N glasses analyzed in this study. The hardness values range from 7.35 to 10.12 GPa and slightly increase with the atomic packing density. A fit of the obtained data to a linear dependence of hardness on compactness yielded $H_v = -10(5) + 32(8) \times [C_g]$, with $R^2 = 0.44$ and the dependence of hardness on N yielded $H_v = 6.52(0.46) + 0.05(0.01) \times [N]$, with $R^2 = 0.53$.

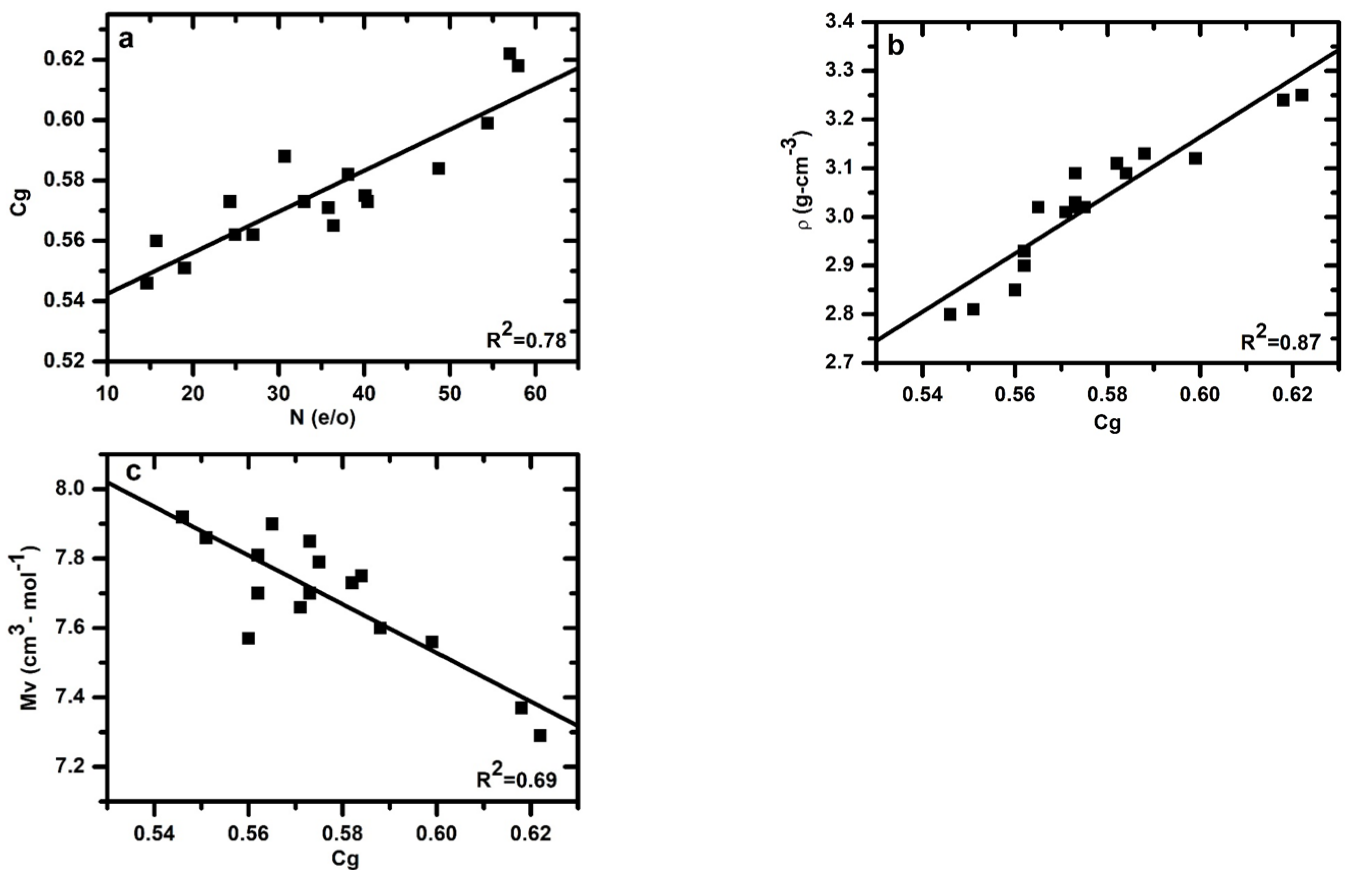


Figure 2. (a) Relation between glass atomic packing density and nitrogen content (b) glass density as a function of glass atomic packing density (c) relation between glass atomic packing density and molar volume of *Ca-Si-O-N* glasses.

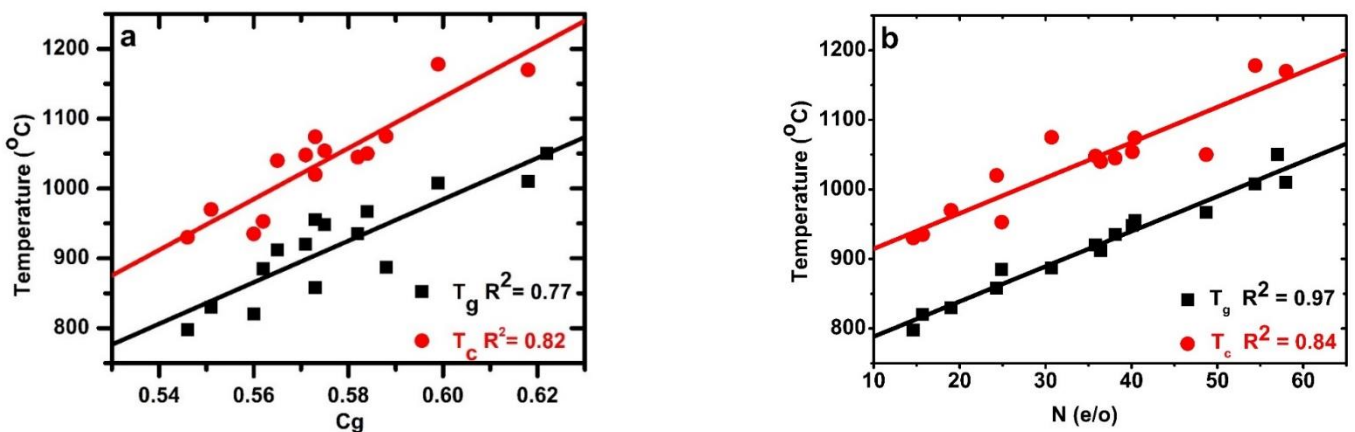


Figure 3. (a) Glass transition and crystallization temperatures as a function of glass atomic packing density (b) glass transition and crystallization temperatures as a function of nitrogen content.

3.6. Effect of Atomic Packing Density on Refractive Index

The RI depends primarily on the polarizability of the various constituent ions of materials and the bonds between atoms. Figure 5a show that there is a substantial increase in RI with the increasing atomic packing density of the glasses. Figure 5b show the relationship between the RI and N content. A fit of the obtained data to a linear dependence of RI on C_g yielded $RI = -0.92(0.25) + 4.62(0.43) \times [C_g]$, with $R^2 = 0.87$ and the dependence of RI on N content yielded $RI = 1.49(0.02) + 0.0072(0.0005) \times [N]$, with $R^2 = 0.91$, indicating

that the C_g and N content have a similar effect on the RI . The strong relationship between the density and RI of Ca–Si–O–N is expected when considering the result of Figure 5c and their corresponding correlation coefficient with $R^2 = 0.77$. Indeed, the refractive index of an oxide-based glass is normally governed by both the atom/ion polarizabilities and the packing density of the constituent atom.

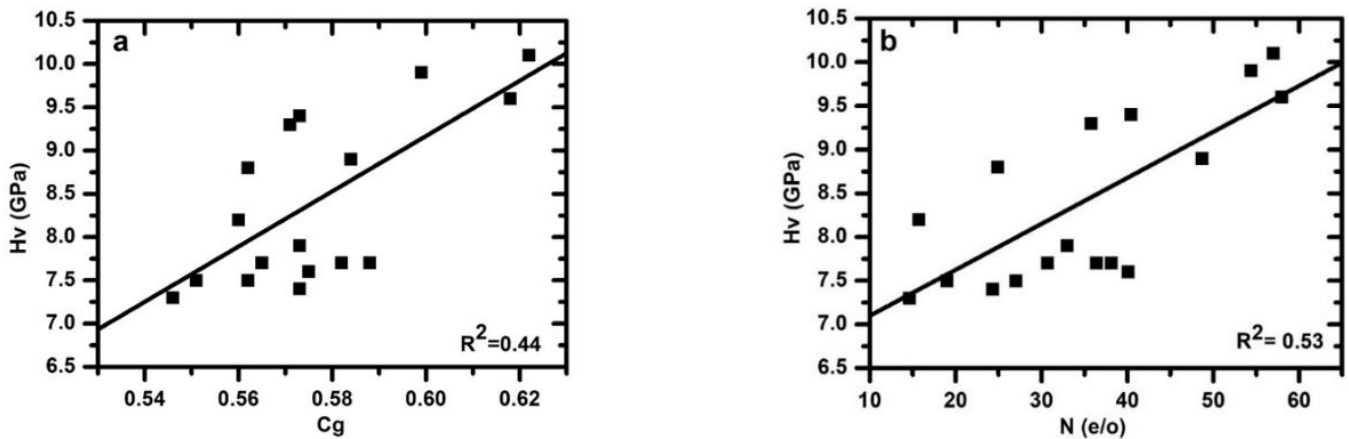


Figure 4. (a) Microhardness as a function of glass atomic packing density (b) microhardness as a function of nitrogen content (in e/o).

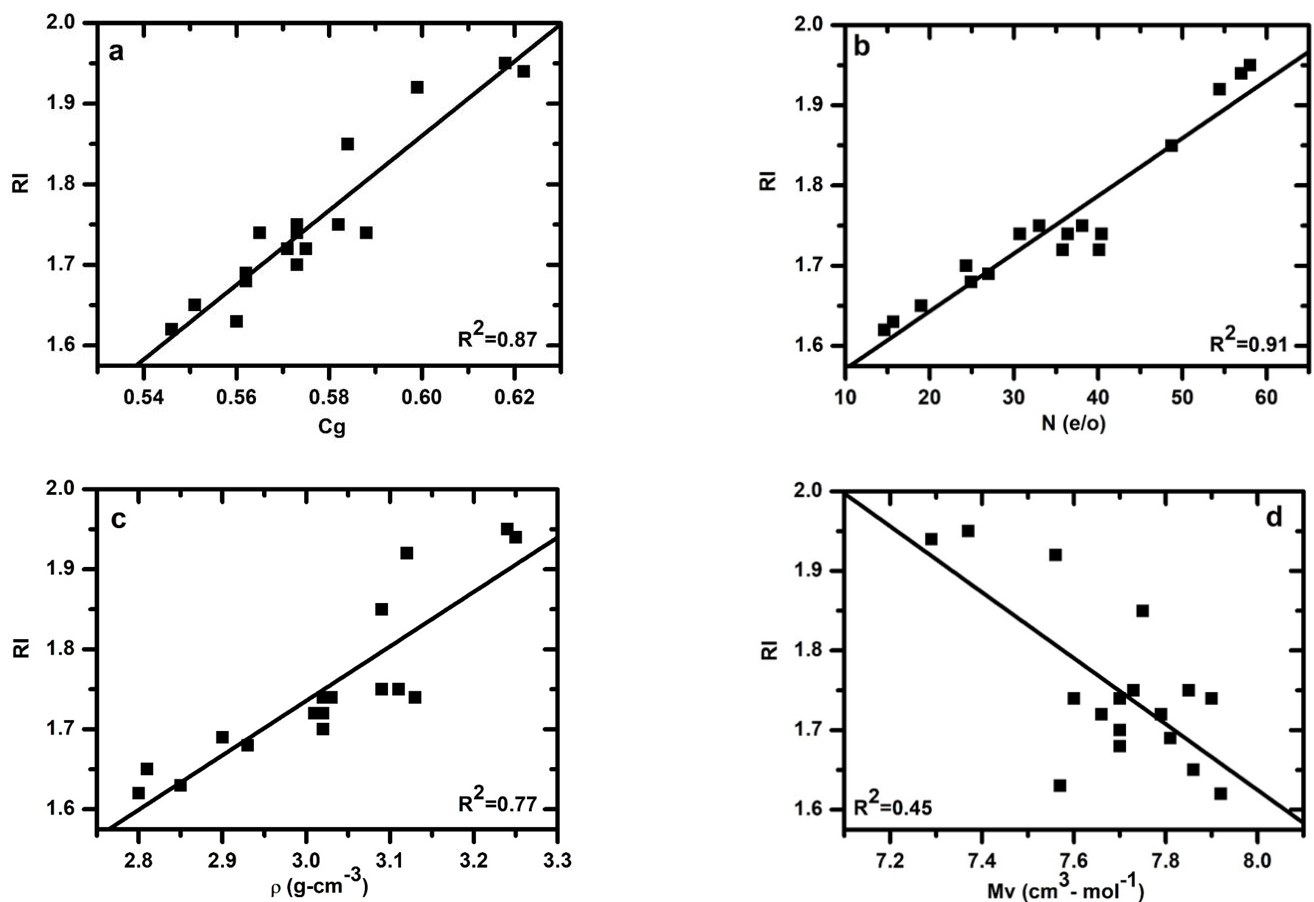


Figure 5. Left panel: (a) Glass refractive index as a function of atomic packing density (c) relation between refractive index and density. Right panel: (b) glass refractive index as a function of nitrogen content (in e/o) (d) relation between refractive index and molar volume for Ca–Si–O–N glasses.

4. Discussion

For most glasses except oxynitride ones, the atomic packing density decreases as the cross-linking degree of the atomic network increases. This is because as the cross-link develops, the glass network becomes less compliant, and the atomic topology is governed more and more by the glass former-oxygen skeleton [34–37]. For instance, C_g is typical of the order of 0.45 for amorphous silica ($n_{BO} = 4$ and $\langle n \rangle = 2.67$), 0.5 for soda–lime–silica glasses (typical window glasses, n_{BO} is between 2 and 3), and above 0.7 for most bulk metallic glasses. In this regard, silicon oxynitride glasses behave anomalously since they exhibit C_g values typically larger than 0.55, although N is supposed to significantly increase the connectivity [27,38]. A striking feature is that C_g increases with the N content in spite of the fact that N is three-fold coordinated. For instance, in the Ca–Si–O–N system [13], the atomic packing density, as well as glass density, increases with the N content, whereas in the Ca–Si–O glass system [39], it was found that the atomic packing density decreases as the Ca content decreases and the number of bridging oxygen increases. Furthermore, glasses in the Ca–Si–O–N system containing SiO_3N groups might accommodate more Ca in sites than the equivalent oxide samples without generating non-bridging oxygen species.

Our observed monotonic increase in density and decrease in the molar volume against the glass atomic packing density mirrors the fact that C_g induces contraction in the glass network. Numerous reports on oxynitride systems, e.g., AE–Si–(Al)–O–N [4,14,15,28,30,40–42] and RE–Si–(Al)–O–N [9,10,23,25,43–49], show that the density is more dependent on the modifier content and concentration than the N content. A linear regression fit on both fractional glass compactness and N content yielded $\rho = 0.24 (0.66) + 4.7 (1.3) \times [C_g] + 0.01(0.01) \times [\text{N}]$ with $R^2 = 0.87$. The data thus indicate that ρ primarily depends on C_g . Conversely, the Mv , which is inversely proportional to density, decreases non-linearly with increasing C_g of the Ca–Si–O–N glasses. The Mv is also affected by modifier cations [7,50–52]. In earlier reports on N-rich oxynitride glasses in the Ca–Si–O–N [12,28], Sr–Si–O–N [14], and Ba–Si–O–N [15] systems, it was found that increasing C_g reduces the Mv and increasing content of modifier cation increases it.

The glass transition temperature (T_g) depends on the chemical composition, atomic packing density, and strength of the cation–anion bonds. Since an increase in N content increases the atomic packing density of glass, the cross-linking of the glass network increases, so the T_g is expected to increase alongside the C_g . The T_g and T_c increase with increasing nitrogen content due to an increase in the coordination of the anion and a stronger covalent bond between Si–N versus Si–O. The increase in T_g with the N content is consistent with alkaline–earth containing oxynitride glasses [4,12,15,26,30,41,50,53–55]. The improvement in T_g originates from the increase of atomic network cross-linking, due to the three-fold coordinated nitrogen and the atomic packing density, despite nitrogen being lighter than oxygen and the Si–O bond being stronger than the Si–N bond. T_g is also affected by CFS, and for high CFS, the effective force attracting anions increases; consequently, the glass network becomes more compact, which results in T_g increase. For example, the glasses in the Mg–Si–O–N system have higher T_g values than in Ca/Sr/Ba–Si–O–N [26] glasses. The regression analysis yielded $T_g = 670 (200) + 5 (1) \times [\text{N}] + 160 (370) \times [C_g]$ with $R^2 = 0.97$. The present data thus indicate that T_g is more dictated by N content as compared to the C_g of the glass.

The microhardness of the oxynitride glass and the silicate-based oxide glass is dictated by many factors such as the bond strength, C_g , and the polymerization/topology of the network of interconnected SiO_4 and AlO_4 tetrahedra [15,20,24,25,27,56–59]. Generally, microhardness diminishes with increasing alkali or alkaline–earth ion content in both oxide and oxynitride glass networks, which cause depolymerization of the network by converting bridging oxygen (n_{BO}) into non-bridging oxygen (n_{NBO}) species [11,26,60]. N is well known in oxynitride glass systems to increase hardness. Hardness has frequently been related to the CFS of the modifier elements and varies substantially with the type of modifier; e.g., Mg- and Ca-containing glasses exhibit higher hardness values than corresponding Sr- and Ba-containing glasses [26,30]. Furthermore, hardness recurrently

increases with the increase in CFS. Generally, the effects of replacing N for O and modifier cation replacement on hardness are independent of each other and additive rather than synergistic. The present data in the Ca–Si–O–N system do not show a clear trend. A fit of the data to linear dependence of hardness on nitrogen and atomic packing density yielded $H_v = 2.8 (9.5) + 0.05 (0.03) \times [N] + 7 (18) \times [C_g]$ with $R^2 = 0.50$. The regression analysis shows that the hardness is more dependent on the N content as compared to the C_g . It is also possible that different atomic packing density values might correspond to the same microhardness because different mechanisms produce the same permanent deformation.

The refractive index (RI) is found to be increased with both increasing N content and changed with the amount of glass modifier. In addition, it was observed that the amount of glass modifier depends on the atomic number of the modifier element. N-rich glasses in the systems AE–Si–O–N with AE = Mg, Ca, Sr, and Ba also show that the RI depends on the N content and the amount and type of modifiers [26]. For the present Ca–Si–O–N glasses, the RI varies between 1.62 and 1.94 and increases linearly with the atomic packing density of the glass. The RI of glass is dependent on the polarizability and molar volume of the glass [61,62]. The addition of cation modifiers in the glasses network leads to a more open structure. Moreover, the addition of cation modifiers causes the glass structure to expand to accommodate the cations at interstitial sites. Therefore, this increase in molar volume, having a considerable effect compared to any polarizability effect, leads to a decrease in the RI , as shown in Figure 5d. The addition of N in the glass network increases structural polymerization. This creates a more rigid network and causes a decrease in the molar volume leading to a higher RI . From the present data, it is clear that RI decreases with increasing Mv . In previous studies of Sr–Si–O–N [14] and Ba–Si–O–N [15] systems, it was found that modifiers are slightly more effective on the RI than the N content. The Ba-containing glasses show high RI values compared to the Sr- and Ca-containing glasses. A fit of the data to a linear dependence of RI on N and atomic packing density yielded $RI = 0.40 (0.33) + 0.0044 (0.0009) \times [N] + 2.08 (0.63) \times [C_g]$ with $R^2 = 0.95$. The present data demonstrate that RI is correlated to both the N content and the C_g of the glass.

5. Conclusions

Physical and optical properties such as glass transition temperature, density, hardness, molar volume, crystallization temperature, and refractive index were studied as a function of atomic packing density for 17 calcium silicon oxynitride glasses with different Ca (15 to 42 e/o) and N (15 to 58 e/o) contents. Glasses in the Ca–Si–O–N matrix with a high atomic packing density exhibit relatively strong interatomic interactions and sturdily affect some properties. The number of bridging oxygen and average coordination number manifested non-linear relationships with the atomic packing density. The density and refractive index are found to increase predominantly with the atomic packing density but also with the Ca content. Indeed, the refractive index of an oxynitride-based glass is normally governed by both the atom/ion polarizabilities and the packing density of the constituent atom. The glass transition and crystallization temperatures and molar volume increase and decrease, respectively, with increasing the atomic packing density. Unexpectedly no strong correlation between the microhardness and atomic packing density of the Ca–Si–O–N glasses was observed, indicating that the atomic packing density is not solely controlled by the underlying deformation mechanism. The regression analysis shows that the microhardness is more dominated by the N content compared to the atomic packing density.

Funding: This research received no external funding.

Institutional Review Board Statement: Not applicable.

Informed Consent Statement: Not applicable.

Data Availability Statement: Not applicable.

Acknowledgments: The author acknowledges Abbas Saeed Hakeem from King Fahd University of Petroleum and Minerals (KFUPM) for his help and constructive suggestions.

Conflicts of Interest: The authors declare no conflict of interest.

References

1. Aujla, R.S.; Lengward, G.; Lewis, M.H.; Seymour, E.F.W.; Styles, G.A.; West, G.W. An NMR-Study of Silicon Coordination in Y-Si-Al-O-N Glasses. *Philos. Mag. B* **1986**, *54*, L51–L56. [[CrossRef](#)]
2. Brow, R.; Pantano, C.; Boyd, D.C. Nitrogen Coordination in Oxynitride Glasses. *J. Am. Ceram. Soc.* **1984**, *67*, c72–c74. [[CrossRef](#)]
3. Loehman, R.E. Preparation and Properties of Oxynitride Glasses. *J. Non-Cryst. Solids*. **1983**, *56*, 123–134. [[CrossRef](#)]
4. Sakka, S.; Kamiya, K.; Yoko, T. Preparation and Properties of Ca-Al-Si-O-N Oxynitride Glasses. *J. Non-Cryst. Solids*. **1983**, *56*, 147–152. [[CrossRef](#)]
5. Sakka, S. Structure, Properties and Application of Oxynitride Glasses. *J. Non-Cryst. Solids*. **1995**, *181*, 215–224. [[CrossRef](#)]
6. Hampshire, S. Oxynitride glasses, their properties and crystallisation—A review. *J. Non-Cryst. Solids*. **2003**, *316*, 64–73. [[CrossRef](#)]
7. Becher, P.F.; Hampshire, S.; Pomeroy, M.J.; Hoffmann, M.J.; Lance, M.J.; Satet, R.L. An Overview of the Structure and Properties of Silicon-Based Oxynitride Glasses. *Int. J. Appl. Glass Sci.* **2011**, *2*, 63–83. [[CrossRef](#)]
8. Ali, S.; Jonson, B.; Pomeroy, M.J.; Hampshire, S. Issues associated with the development of transparent oxynitride glasses. *Ceram. Int.* **2015**, *41*, 3345–3354. [[CrossRef](#)]
9. Hakeem, A.S.; Grins, J.; Esmailzadeh, S. La-Si-O-N glasses—Part I. Extension of the glass forming region. *J. Eur. Ceram. Soc.* **2007**, *27*, 4773–4781. [[CrossRef](#)]
10. Hakeem, A.S.; Grins, J.; Esmailzadeh, S. La-Si-O-N glasses—Part II: Vickers hardness and refractive index. *J. Eur. Ceram. Soc.* **2007**, *27*, 4783–4787. [[CrossRef](#)]
11. Leonova, E.; Hakeem, A.S.; Jansson, K.; Stevansson, B.; Shen, Z.; Grins, J.; Esmailzadeh, S.; Edén, M. Nitrogen-rich La-Si-Al-O-N oxynitride glass structures probed by solid state NMR. *J. Non-Cryst. Solids*. **2008**, *354*, 49–60. [[CrossRef](#)]
12. Sharafat, A.; Grins, J.; Esmailzadeh, S. Glass-forming region in the Ca–Si–O–N system using CaH₂ as Ca source. *J. Eur. Ceram. Soc.* **2008**, *28*, 2659–2664. [[CrossRef](#)]
13. Sharafat, A. *Preparation, Characterization and Properties of Nitrogen Rich Glasses in Alkaline Earth-Si-O-N Systems*; Institutionen för Fysikalisk Kemi, Organisk Kemi och Strukturkemi: Stockholm, Sweden, 2009; p. 116.
14. Sharafat, A.; Forslund, B.; Grins, J.; Esmailzadeh, S. Formation and properties of nitrogen-rich strontium silicon oxynitride glasses. *J. Mater. Sci.* **2009**, *44*, 664–670. [[CrossRef](#)]
15. Ali, S.; Jonson, B. Glasses in the Ba-Si-O-N System. *J. Am. Ceram. Soc.* **2011**, *94*, 2912–2917. [[CrossRef](#)]
16. Ali, S. Elastic Properties and Hardness of Mixed Alkaline Earth Silicate Oxynitride Glasses. *Materials* **2022**, *15*, 5022. [[CrossRef](#)]
17. Acikgoz, A.; Demircan, G.; Yilmaz, D.; Aktas, B.; Yalcin, S.; Yorulmaz, N. Structural, mechanical, radiation shielding properties and albedo parameters of alumina borate glasses: Role of CeO₂ and Er₂O₃. *Mater. Sci. Eng. B* **2022**, *276*, 115519. [[CrossRef](#)]
18. Aktas, B.; Acikgoz, A.; Yilmaz, D.; Yalcin, S.; Dogru, K.; Yorulmaz, N. The role of TeO₂ insertion on the radiation shielding, structural and physical properties of borosilicate glasses. *J. Nucl. Mater.* **2022**, *563*, 153619. [[CrossRef](#)]
19. Fidan, M.; Acikgoz, A.; Demircan, G.; Yilmaz, D.; Aktas, B. Optical, structural, physical, and nuclear shielding properties, and albedo parameters of TeO₂–BaO–B₂O₃–PbO–V₂O₅ glasses. *J. Phys. Chem. Solids* **2022**, *163*, 110543. [[CrossRef](#)]
20. Kohli, J.T.; Shelby, J.E. Formation and Properties of Rare-Earth Aluminosilicate Glasses. *Phys. Chem. Glasses* **1991**, *32*, 67–71.
21. Tanabe, S.; Hirao, K.; Soga, N. Elastic Properties and Molar Volume of Rare-Earth Aluminosilicate Glasses. *Am. Ceram. Soc.* **1992**, *75*, 503–506. [[CrossRef](#)]
22. Murakami, Y.; Yamamoto, H. Properties of Oxynitride Glasses in the Ln-Si-Al-O-N Systems (Ln = Rare-Earth). *Nippon. Seramikkusu Kyokai Gakujutsu Ronbunshi-J. Ceram. Soc. Jpn.* **1994**, *102*, 231–236. [[CrossRef](#)]
23. Ohashi, M.; Nakamura, K.; Hirao, K.; Kanzaki, S. Formation and Properties of Ln-Si-O-N Glasses (Ln = Lanthanides or Y). *J. Am. Ceram. Soc.* **1995**, *78*, 71–76. [[CrossRef](#)]
24. Ramesh, R.; Nestor, E.; Pomeroy, M.J.; Hampshire, S. Formation of Ln-Si-Al-O-N glasses and their properties. *J. Eur. Ceram. Soc.* **1997**, *17*, 1933–1939. [[CrossRef](#)]
25. Becher, P.F.; Waters, S.B.; Westmoreland, C.G.; Riester, L. Compositional effects on the properties of Si-Al-Re-based oxynitride glasses (RE = La, Nd, Gd, Y, or Lu). *J. Am. Ceram. Soc.* **2002**, *85*, 897–902. [[CrossRef](#)]
26. Sharafat, A.; Bo, J. Compositional effects on the properties of high nitrogen content alkaline-earth silicon oxynitride glasses, AE = Mg, Ca, Sr, Ba. *J. Eur. Ceram. Soc.* **2011**, *31*, 611–618.
27. Rouxel, T. Elastic properties and short-to medium-range order in glasses. *J. Am. Ceram. Soc.* **2007**, *90*, 3019–3039.
28. Sharafat, A.; Grins, J.; Esmailzadeh, S. Hardness and refractive index of Ca-Si-O-N glasses. *J. Non-Cryst. Solids* **2009**, *355*, 301–304. [[CrossRef](#)]
29. Shannon, R.D. Revised Effective Ionic-Radii and Systematic Studies of Interatomic Distances in Halides and Chalcogenides. *Acta Cryst. A* **1976**, *32*, 751–767. [[CrossRef](#)]
30. Pastuszak, R.; Verdier, P. M-Si-Al-O-N Glasses (M = Mg, Ca, Ba, Mn, Nd), Existence Range and Comparative-Study of Some Properties. *J. Non-Cryst. Solids* **1983**, *56*, 141–146. [[CrossRef](#)]

31. Desmaitsonbrut, M.; Desmaitson, J. The Reactivity in Oxygen of 2 Ca-Si-Al-O-N, Mn-Si-Al-O-N Oxynitride Glasses. *Solid State Ion.* **1988**, *26*, 153.
32. Desmaitsonbrut, M.; Desmaitson, J.; Verdier, P. Oxidation Behavior of an Oxynitride Glass in the System Ca-Si-Al-O-N. *J. Non-Cryst. Solids* **1988**, *105*, 323–329. [[CrossRef](#)]
33. Sharafat, A.; Berastegui, P.; Esmailzadeh, S.; Eriksson, L.; Grins, J. A cubic calcium oxynitrido-silicate, $\text{Ca}_{2.89}\text{Si}_2\text{N}_{1.76}\text{O}_{4.24}$. *Acta Crystallogr. Sect. E Struct. Rep. Online* **2011**, *67*, i66. [[PubMed](#)]
34. Rouxel, T.; Dely, N.; Sangleboeuf, J.C.; Deriano, S.; LeFloch, M.; Beuneu, B.; Hampshire, S. Structure-property correlations in Y-Ca-Mg-sialon glasses: Physical and mechanical properties. *J. Am. Ceram. Soc.* **2005**, *88*, 889–896.
35. Sellappan, P.; Sharafat, A.; Keryvin, V.; Houizot, P.; Rouxel, T.; Grins, J.; Esmailzadeh, S. Elastic properties and surface damage resistance of nitrogen-rich (Ca,Sr)-Si-O-N glasses. *J. Non-Cryst. Solids* **2010**, *356*, 2120–2126.
36. Lv, P.; Wang, C.; Svensson, B.; Yu, Y.; Wang, T.; Edén, M. Impact of the cation field strength on physical properties and structures of alkali and alkaline-earth borosilicate glasses. *Ceram. Int.* **2022**, *48*, 18094–18107.
37. Pönitzsch, A.; Nofz, M.; Wondraczek, L.; Deubener, J. Bulk elastic properties, hardness and fatigue of calcium aluminosilicate glasses in the intermediate-silica range. *J. Non-Cryst. Solids* **2016**, *434*, 1–12.
38. Rouxel, T. What we can learn from crystals about the mechanical properties of glass. *J. Ceram. Soc. Jpn.* **2022**, *130*, 519–530.
39. Deriano, S.; Rouxel, T.; LeFloch, M.; Beuneu, B. Structure and mechanical properties of alkali-alkaline earth-silicate glasses. *Phys. Chem. Glasses* **2004**, *45*, 37–44.
40. Homeny, J.; Mcgarry, D.L. Preparation and Mechanical-Properties of Mg-Al-Si-O-N Glasses. *J. Am. Ceram. Soc.* **1984**, *67*, C225–C227.
41. Sharafat, A.; Grins, J.; Esmailzadeh, S. Properties of high nitrogen content mixed alkali earth oxynitride glasses ($\text{AE}_{(x)}\text{Ca}_{(1-x)}(1.2(1))\text{SiO}_{1.9(1)}\text{N}_{0.86(6)}$, AE = Mg, Sr, Ba). *J. Non-Cryst. Solids* **2009**, *355*, 1259–1263.
42. Gueguen, Y.; Sharafat, A.; Grins, J.; Rouxel, T. Viscosity of high-nitrogen content Ca-Si-O-N glasses. *J. Am. Ceram. Soc.* **2010**, *30*, 3455–3458.
43. Denisse, C.M.M.; Troost, K.Z.; Elferink, J.B.O.; Habraken, F.H.P.M.; van der Weg, W.F.; Hendriks, M. Plasma-enhanced growth and composition of silicon oxynitride films. *J. Appl. Phys.* **1986**, *60*, 2536–2542.
44. Hampshire, S.; Nestor, E.; Flynn, R.; Besson, J.L.; Rouxel, T.; Lemercier, H.; Goursat, P.; Sebai, M.; Thompson, D.P.; Liddell, K. Yttrium Oxynitride Glasses—Properties and Potential for Crystallization to Glass-Ceramics. *J. Eur. Ceram. Soc.* **1994**, *14*, 261–273.
45. Menke, Y.; Peltier-Baron, V.; Hampshire, S. Effect of rare-earth cations on properties of sialon glasses. *J. Non-Cryst. Solids* **2000**, *276*, 145–150.
46. Becher, P.F.; Ferber, M.K. Temperature-Dependent Viscosity of SiREAl-Based Glasses as a Function of N:O and RE:Al Ratios (RE = La, Gd, Y, and Lu). *J. Am. Ceram. Soc.* **2004**, *87*, 1274–1279.
47. Hampshire, S.; Pomeroy, M.J. Effect of composition on viscosities of rare earth oxynitride glasses. *J. Non-Cryst. Solids* **2004**, *344*, 1–7.
48. Lofaj, F.; Deriano, S.; LeFloch, M.; Rouxel, T.; Hoffmann, M.J. Structure and rheological properties of the RE-Si-Mg-O-N (RE = Sc, Y, La, Nd, Sm, Gd, Yb and Lu) glasses. *J. Non-Cryst. Solids* **2004**, *344*, 8–16.
49. Lofaj, F.; Satet, R.; Hoffmann, M.J.; de Lopez, A.R. Thermal expansion and glass transition temperature of the rare-earth doped oxynitride glasses. *J. Eur. Ceram. Soc.* **2004**, *24*, 3377–3385.
50. Hampshire, S.; Hanifi, A.R.; Genson, A.; Pomeroy, M.J. Ca-Si-Al-O-N glasses: Effects of fluorine on glass formation and properties. *Key. Eng. Mater.* **2007**, *352*, 165–172.
51. Iftekhhar, S.; Pahari, B.; Okhotnikov, K.; Jaworski, A.; Svensson, B.; Grins, J.; Edén, M. Properties and Structures of $\text{RE}_2\text{O}_3\text{-Al}_2\text{O}_3\text{-SiO}_2$ (RE = Y, Lu) Glasses Probed by Molecular Dynamics Simulations and Solid-State NMR: The Roles of Aluminum and Rare-Earth Ions for Dictating the Microhardness. *J. Phys. Chem. C* **2012**, *116*, 18394–18406.
52. Bäck, L.G.; Ali, S.; Karlsson, S.; Möncke, D.; Kamitsos, E.I.; Jonson, B. Mixed alkali/alkaline earth-silicate glasses: Physical properties and structure by vibrational spectroscopy. *Int. J. Appl. Glass Sci.* **2019**, *10*, 349–362. [[CrossRef](#)]
53. Tredway, W.K.; Risbud, S.H. Melt Processing and Properties of Barium-Sialon Glasses. *J. Am. Ceram. Soc.* **1983**, *66*, 324–327. [[CrossRef](#)]
54. Hanada, T.; Naotaka, U.; Naohire, S. Preparation, properties and bond character of nitrogen in calcium silicon oxynitride glasses. *J. Ceram. Soc. Jpn.* **1988**, *96*, 281–289. [[CrossRef](#)]
55. Hanifi, A.R.; Genson, A.; Pomeroy, M.J.; Hampshire, S. An introduction to the glass formation and properties of Ca-Si-Al-O-N-F glasses. *Mater. Sci. Forum* **2007**, *554*, 17–23. [[CrossRef](#)]
56. Lemercier, H.; Rouxel, T.; Fargeot, D.; Besson, J.L.; Piriou, B. Yttrium SiAlON glasses: Structure and mechanical properties—Elasticity and viscosity. *J. Non-Cryst. Solids* **1996**, *201*, 128–145. [[CrossRef](#)]
57. Zheng, Q.J.; Potuzak, M.; Mauro, J.C.; Smedskjaer, M.M.; Youngman, R.E.; Yue, Y.Z. Composition-structure-property relationships in boroaluminosilicate glasses. *J. Non-Cryst. Solids* **2012**, *358*, 993–1002. [[CrossRef](#)]
58. García-Bellés, Á.R.; Monzó, M.; Barba, A.; Clausell, C.; Pomeroy, M.J.; Hanifi, A.R.; Hampshire, S. Factors Controlling Properties of Ca-Mg, Ca-Er, Ca-Nd, or Ca-Y-Modified Aluminosilicate Glasses Containing Nitrogen and Fluorine. *J. Am. Ceram. Soc.* **2013**, *96*, 2839–2845. [[CrossRef](#)]
59. Hakeem, A.S.; Ali, S.; Jonson, B. Preparation and properties of mixed La-Pr silicate oxynitride glasses. *J. Non-Cryst. Solids* **2013**, *368*, 93–97. [[CrossRef](#)]

60. Iftekhar, S.; Grins, J.; Edén, M. Composition–property relationships of the $\text{La}_2\text{O}_3\text{–Al}_2\text{O}_3\text{–SiO}_2$ glass system. *J. Non-Cryst. Solids* **2010**, *356*, 1043–1048. [[CrossRef](#)]
61. Coon, D.N.; Doyle, T.E.; Weidner, J.R. Refractive-Indexes of Glasses in the Y-Al-Si-O-N System. *J. Non-Cryst. Solids* **1989**, *108*, 180–186. [[CrossRef](#)]
62. Dimitrov, V.; Komatsu, T. Electronic polarizability, optical basicity and non-linear optical properties of oxide glasses. *J. Non-Cryst. Solids* **1999**, *249*, 160–179. [[CrossRef](#)]